THE JOURNAL OF PHYSICAL CHEMISTRY B

Article

Molecular Mechanism Behind Solvent Concentration Dependent Optimal Activity of Thermomyces Lanuginosus Lipase in Biocompatible Ionic Liquid: Interfacial Activation Through Arginine Switch

Sudip Das, Tarak Karmakar, and Sundaram Balasubramanian

J. Phys. Chem. B, **Just Accepted Manuscript** • DOI: 10.1021/acs.jpcb.6b08534 • Publication Date (Web): 25 Oct 2016

ACS Publications

The Journal of Physical Chemistry B is published by the American Chemical Society. 1155 Sixteenth Street N.W., Washington, DC 20036

Molecular Mechanism behind Solvent Concentration Dependent Optimal Activity of Thermomyces Lanuginosus Lipase in Biocompatible Ionic Liquid: Interfacial Activation through Arginine Switch

Sudip Das, Tarak Karmakar and Sundaram Balasubramanian*

Chemistry and Physics of Materials Unit

Jawaharlal Nehru Centre for Advanced Scientific Research, Bangalore 560 064, India

E-mail: bala@jncasr.ac.in

*To whom correspondence should be addressed

Abstract

Thermomyces lanuginosus lipase (TLL) is an industrially significant catalyst for the production of biodiesel due to its operability over a wide range of pH and temperature. Molecular dynamics simulations of TLL in aqueous solutions of a *biocompatible* ionic liquid (IL), cholinium glycinate (ChGly) have been carried out to investigate the microscopic reasons for the experimentally observed enhancement in the activity of TLL, upon addition of room temperature IL, especially at an optimal concentration. Eight different TLL systems in both its open and closed forms at various concentrations of the room temperature IL in water have been studied. A special orientation of the lid residue W89 in the closed form that enables an optimal substrate binding rate has been identified which can be probed via fluorescence spectroscopy. The flipping and consequent exposure of W89 in the open form of TLL induces a change in the lid helicity and orientation in such a way that the residue R84 from the front lid hinge gets trapped around a particular region in all the systems except at 0.5M concentration of IL. In the latter, R84 exhibits considerable fluxionality and moves back and forth via a water channel which is formed due to the chaotropic nature of cholinium cation. *Arginine switch* is well established to be the primary signature of interfacial activation of TLL, one that is observed here in an *optimal IL concentration* (0.5M) without the use of substrate or surfactant. The present work can pave for the development of a broader platform for the understanding and application of lipases in *environment-friendly* catalysis.

Introduction

As the world passes through an era of increasing demand for energy and diminishing supplies of fossil fuels, newer sources need to be explored. In this context, along with other unconventional sources, the production of biodiesel fuel (fatty acid alkyl ester) from animal and plant oils has drawn much attention of researchers in the fields of chemical, biochemical and protein engineering.[1–4] Lipases are a class of enzymes found to be most suitable for biodiesel production due to their unique feature called *interfacial activation*.[1,4–7]

In the course of interfacial activation of a lipase, buried hydrophobic side chains of amphiphilic lid residues get exposed and stick to the lipid-solvent interface. Such an "activation" of the enzyme is naturally favored in a solvent possessing either a hydrophobic character or a low dielectric constant.[8–11] The separation and purification of product too become easier in such interfacially immobilized enzymatic catalysis (immobilized on large hydrophobic surface of aggregated substrate or surfactant), than when the reaction is carried out with chemical catalysts.[1,5–7] Among all lipases, the ones from the thermophilic fungus *Thermomyces lanuginosus* (TL) are found to be industrially significant catalysts for biodiesel production,[4] owing to their inherent stability at high temperature,[12] a wide range of pH operating conditions[13] as well as high methanolysis activity.[14–17] TL lipase (TLL) has been used not only in biodiesel production but also in food industry, in enantiomeric separation of racemic mixtures and in many regio-selective or specific processes to synthesize fine chemicals.[4] Rightfully, TLL has been studied by several researchers through *in vitro* experiments,[18] site-directed mutagenesis,[19–21] X-ray crystal structures,[22,23] site-directed spin labeling,[24] intrinsic tryptophan fluorescence studies,[20,25–27] and molecular dynamics simulations.[19,28,29]

TLL has a typical α/β hydrolase fold,[22,23] maintained by three disulfide linkages (C268-C22, C36-C41 and C104-C107).[23] Like all other lipases, a flexible lid (residues 86-92) covers (uncovers) the active site in the closed (open) form of the enzyme.[17] The active site of the enzyme contains a trypsin-like S146-H258-D201 catalytic triad.[30] The open-closed motion of the lid is governed by two hinge regions (residues 82-85 and 93-96) proximal to the

lid.[30] Crystallographic studies[23] have shown that in the course of interfacial activation with increasing lipid concentration or decreasing solvent polarity, C268-C22 disulfide isomerization and formation of a short α_0-helix (residues 23-28) followed by the lid residue R84 switch from D57 to C268, convert TLL from its catalytically low activity (LA) closed state (Protein Data Bank or PDB ID: 1DT3) to activated (A) closed form (PDB ID: 1DT5) (Figures 1 and 2 top). In the subsequent step of interfacial activation, the opening of the lid converts this activated (A) closed form to fully activated (FA) open form (PDB ID: 1DTE) (Figures 1 and 2 top).

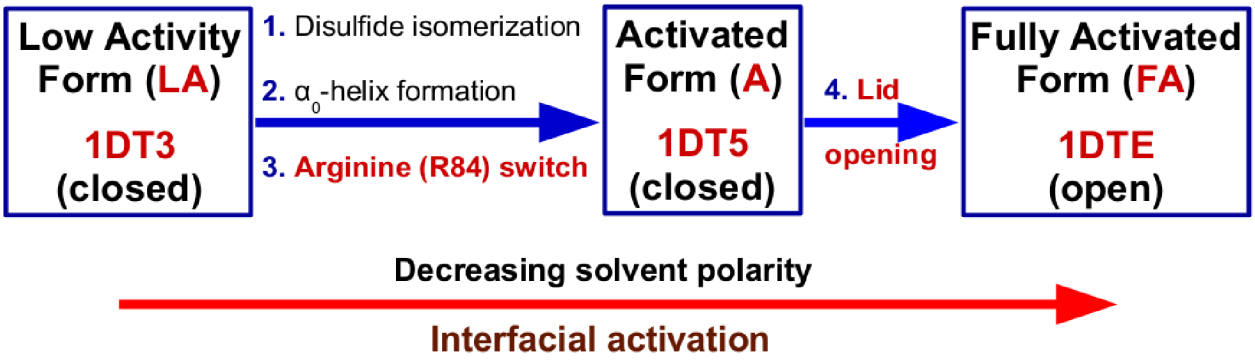

Figure 1: Key changes in the structure of TLL during interfacial activation as proposed by Brzozowski *et al.*[23] 1DT3, 1DT5 and 1DTE are PDB IDs.

Biocatalysis of lipases is preferably performed in less polar organic media (mainly alcohol) or in aqueous organic solutions (where the extent of interfacial activation is more) rather than in highly polar, aqueous media.[31] However, several reports in the literature[32–37] have also suggested alcohol to cause the inactivation and/or thermal destabilization of the enzyme. A very recent simulation study of TLL in methanol solvent has explored the details of the molecular mechanism behind this inactivation.[19]

One of the ways to overcome this type of inactivation, without losing the advantages of faster lid opening in less polar solutions compared to pure water, is to substitute the organic component by less volatile ionic liquid (IL). The low volatility of ILs will allow the catalysis to be performed at higher than ambient temperatures, which in turn increases the catalytic rate. ILs can be constituted by a proper combination of cation and anion

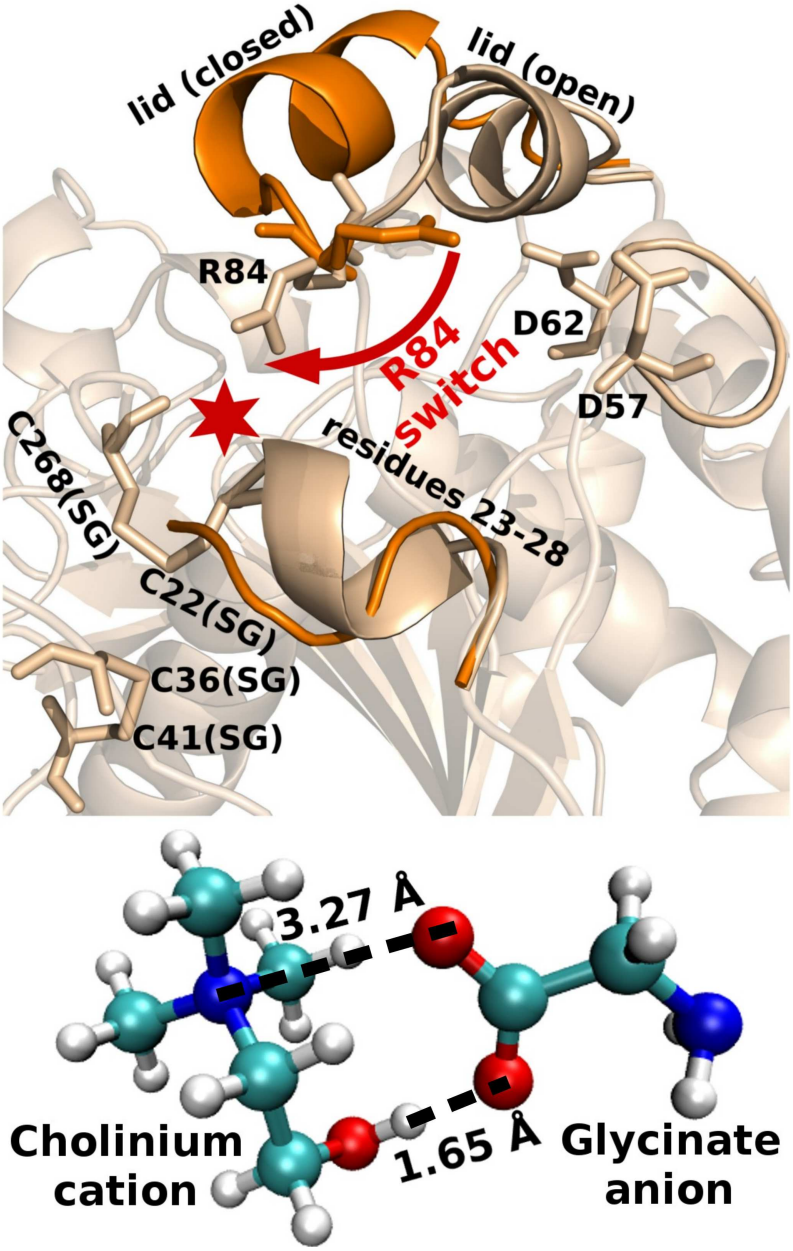

Figure 2: **Top:** The overlay of low activity closed (1DT3) (orange) and fully activated open (1DTE) (wheat) crystal structures of TLL highlighting the zones related to interfacial activation. The red asterisk represents the position of the active site. The red arrow shows the direction of arginine (R84) switch. **Bottom:** Geometry optimized cholinium glycinate (ChGly) ion pair in gas phase. Dotted lines show the distance between corresponding atoms.

chosen from around 10^6 possible combinations.[38,39] Like polar organic solvents, ILs can also form water-mimicking hydrogen bonding network around the protein surface residues that stabilize the native fold of the protein.[40–42] ILs with proper cation-anion combination can also prevent TLL (which has a strong tendency to form ordered biomolecular aggregates confronting its open active centers[43]) from forming disordered aggregates during folding.[42] All these features make ILs a novel media for proteins in diverse biotechnological applications. There are several studies[44–52] and reviews[53–55] in literature on the influence of different ILs on the activity of lipases. Over the last decade, applications of room temperature ILs (RTILs) in biocatalysis for biofuel production has become an emerging field of research.[2,3,56–61]

A very recent experimental study of TLL catalyzed hydrolysis of *p*-nitrophenyl esters at optimum temperature and pH by Deive *et al.* showed an enhancement (up to 50%) of enzymatic activity in aqueous cholinium amino acid (ChAA) IL solvents compared to pure water.[62] They also observed that among the ChAA ILs, TLL showed its highest activity in ChGly (Figure 2 bottom). The activity was observed to reach a maximum at a particular concentration of IL (around 0.5M) and decreased on increasing IL concentration further. However, this observation is in apparent contradiction to the interfacial activation of lipases, as the rate of interfacial activation increases with increase in IL concentration, i.e. with a decrease in solvent polarity.[23] Thus, a comprehensive microscopic explanation for these interesting observations needs to be offered.

In the present study, the structural changes of TLL at varying concentrations of ChGly IL in water are studied. Due to the biocompatibility, ecotoxicity[63] and miscibility with water,[64] ChAA ILs have established themselves to be one of the best possible biocompatible media for biocatalytic applications. The choice of glycinate is justified because of its lack of any (alkyl) side chain which otherwise leads to solvent hydrophobicity-induced destabilization and reduced activation of the enzyme.[65]

In this article, we successfully relate the special interfacial activation mechanism of TLL[23] as obtained from X-ray crystallographic analysis to results obtained from molecular dynamics

simulations of this enzyme in aqueous IL solutions. We propose that the extent of arginine switch (lid residue R84) is the key process behind the experimentally observed[62] optimum solvent-dependent activity of TLL. Our computational findings along with the experimental observations[62] can open up new routes for designing the best possible combination of thermophilic lipases and biocompatible ILs at an optimum solvent concentration which can advance the study and applications of enzymatic catalysis.

Computational Details

1. Choice of crystal structures

In the present study, the X-ray crystal structures of the A and FA forms of TLL (PDB ID: 1DT5 and 1DTE, respectively[23]) were taken from Protein Data Bank (www.rcsb.org) to represent the closed and open forms, respectively. The choice of 1DT5 over 1DT3 for the closed form lies in their crystallization condition. The conditions employed in our simulations (at most 2.0M ChGly in aqueous solvent), corresponds to low ionic strength and thus TLL in its closed form will have a structure which is similar to that of 1DT5 (A) which too has been crystallized under low ionic strength conditions. In contrast, 1DT3 form has been crystallized under high ionic strength condition. The chosen crystal structures were protonated at neutral pH using pdb2gmx tool within GROMACS package.[66–71]

2. Protein-IL system preparation

In the first step, the enzyme was solvated in water. The resulting system was then neutralized by sodium ions and energy minimized. Subsequently, the protein along with the sodium ions, collected from the previous step, was re-solvated in a pre-equilibrated IL-water mixture solution at four different concentrations, 0.0M (pure water), 0.5M, 1.0M and 2.0M, using PACKMOL software [72] (initially in a cubic box of 100 Å edge length). At each concentration, TLL was chosen in both open and closed forms, and thus we simulated a total of eight systems

(four each for the open and closed forms). Details of the systems simulated are summarized in Table S1.

3. Force-field parameters and simulation details

CHARMM36 parameters for the protein and CHARMM general force field (CGenFF)[73,74] parameters for the IL were used along with the TIP3P model[75] for the water molecules. Ions of the IL have been known to be influenced by charge transfer and polarization effects, which can be captured in an effective force field[76–78] by using ion charges which are lesser than unity. Following literature,[79] the ion charges were scaled down so that the cation and the anion have +0.85 and −0.85 charges, respectively. With the reduced charges and CGenFF parameters, simulations of the pure ChGly provided a density which was underestimated by less than 1% of the experimental value (for details, see "Force field parameterization for ChGly IL" in SI). For all systems, a steepest descent energy minimization followed by 1 ns of NVT equilibration (at 300 K) were carried out with position restraints on the heavy atoms of the enzyme with a force constant of 10^3 kcal/mol/rad^2. The imposed restraints were then gradually removed in four successive stages of NPT equilibrations (first three steps were of 0.5 ns each) with force constants 10^3, 10^2, 10^1 and 0 (i.e. unrestrained) kcal/mol/rad^2. The unrestrained NPT equilibration run was performed until the box length converged. Later, for each system, NVT production run was carried out for 120 ns without any constraint. For all NVT runs, the Bussi-Donadio-Parrinello velocity rescaling thermostat[80] with coupling constant 0.5 and 1.0 ps for equilibration and production, respectively at 300 K and for all NPT run, Nosé-Hoover thermostat[81,82] and Parrinello-Rahman barostat[83,84] with coupling constant 1.0 ps for both at 300 K and 1 bar respectively were used. An integration time step of 0.5 fs was used. Particle mesh Ewald (PME) method[85] with cutoff distance of 12 Å was used to treat the long-range electrostatic interactions. The Lennard-Jones (LJ) interactions were smoothly brought down to zero from 10 to 12 Å using the force-switched approach. All systems were simulated using GROMACS 5.0.5 (double precision).[66–71] Trajectories were

visualized using VMD software.[86] Root mean square deviation and fluctuation (RMSD and RMSF), radial distribution function (RDF), the radius of gyration, etc. were calculated using the corresponding routines in GROMACS to analyze trajectories. PyMOL software[87] was used to prepare the graphics.

Results and Discussion

Unless stated otherwise, results from simulations of the open form of the enzyme (PDB ID: 1DTE, Figure 2 top) will be discussed here.

1. Overall conformational changes in TLL

1.1. RMSD and RMSF

To study the overall structural changes of TLL induced by the presence of IL, we have calculated its backbone RMSD (root mean square deviation) and all-atom RMSF (root mean square fluctuation) (averaged over each residue) with respect to the minimized (in water) structure of the enzyme, in its open form. After 100 ns of simulation, the RMSD of all the systems become stable (Figure 3(a)). In the 100-120 ns time window, open_0.5IL and open_1.0IL systems (abbreviated system name, see Table S1 in SI for detail) show higher RMSD values than that in pure water, whereas the open_2.0IL system has RMSD lower than that in pure water.

The RMSF of some lid residues and residues 244-250 are observed to be high (Figure 3(b)). The significantly high RMSF value of R84 in open_0.5IL system (Figure 3(c)) can be attributed to an interesting event, *viz.* arginine switch, which will be discussed in detail later. In all the systems, hydrogen bonds between the lid back hinge residues (residues 93-96) and the nearby protein residues (such as N94-H110 and N96-D111) with an average distance within 2.8-3.0 Å exist; however, the situation in the open_0.5IL system is different. Instead of forming intra-protein hydrogen bonds, the lid back hinge residues (Figure 3(d)) interact

chiefly with the solvent molecules which leads to higher RMSF of the former, compared to that in other systems. This higher RMSF of residue R84 from front hinge (residues 82-85) of active site lid (residues 86-92) and the whole back hinge (residues 93-96) in open_0.5IL system (Figure 3(d)) signifies rigid body hinge-type motion for lid opening and closing; this motion is much simpler than that of the lid opening through the motion of middle region (residue 86-92) of the lid[22,88] (shown in Figure S1). As direct interactions of protein surface residues with water are most favorable for open_0.5IL system (as discussed later), the residues 244-250, being a part of the large random loop in the C-terminal region can easily interact with solvent in this system which leads to its high RMSF (Figure 3(b)), as especially seen in between 80-100 ns of the simulation trajectory (see Figure S2). This is the main reason behind the very high RMSD of TLL in the open_0.5IL system in this time window.

In the *closed form of the lipase*, the hydrophobic residues get buried away from the solvent, and hydrophilic residues get exposed to it (i.e., just opposite to what happens in interfacial activation)[8–10](Figure S3). Due to this, in the closed form of TLL, the lid hydrophobic residues come in close contact with the hydrophobic residues present in a nearby random loop (residues 202-211)(Figure S3). As a result of this hydrophobic interaction, the lid always remains in closed form, independent of the IL concentration (Figure S4). This induces stability to the protein which is reflected in the lower RMSD of overall protein compared to that for the open form of TLL (Figure S5(a)). Again, compared to the open form, the lid comes quite close to the random loop comprising of residues 202-211 in the closed_0.5IL system which leads to strongest hydrophobic interaction between the lid and that random loop, amongst all systems. Residue R84 thus gets locked to C268, whereas it is not locked to any residue in rest of the systems in the closed form of TLL (Figures S6 and S7). This observation is also supported by the RMSF plot (Figure S5(c)) where R84 exhibits the least fluctuation for closed_0.5IL system. All these observations make TLL be most stable in the closed_0.5IL system among all the eight systems, as indicated by the lowest RMSD of TLL in this system (Figure 3(a) and S5(a)).

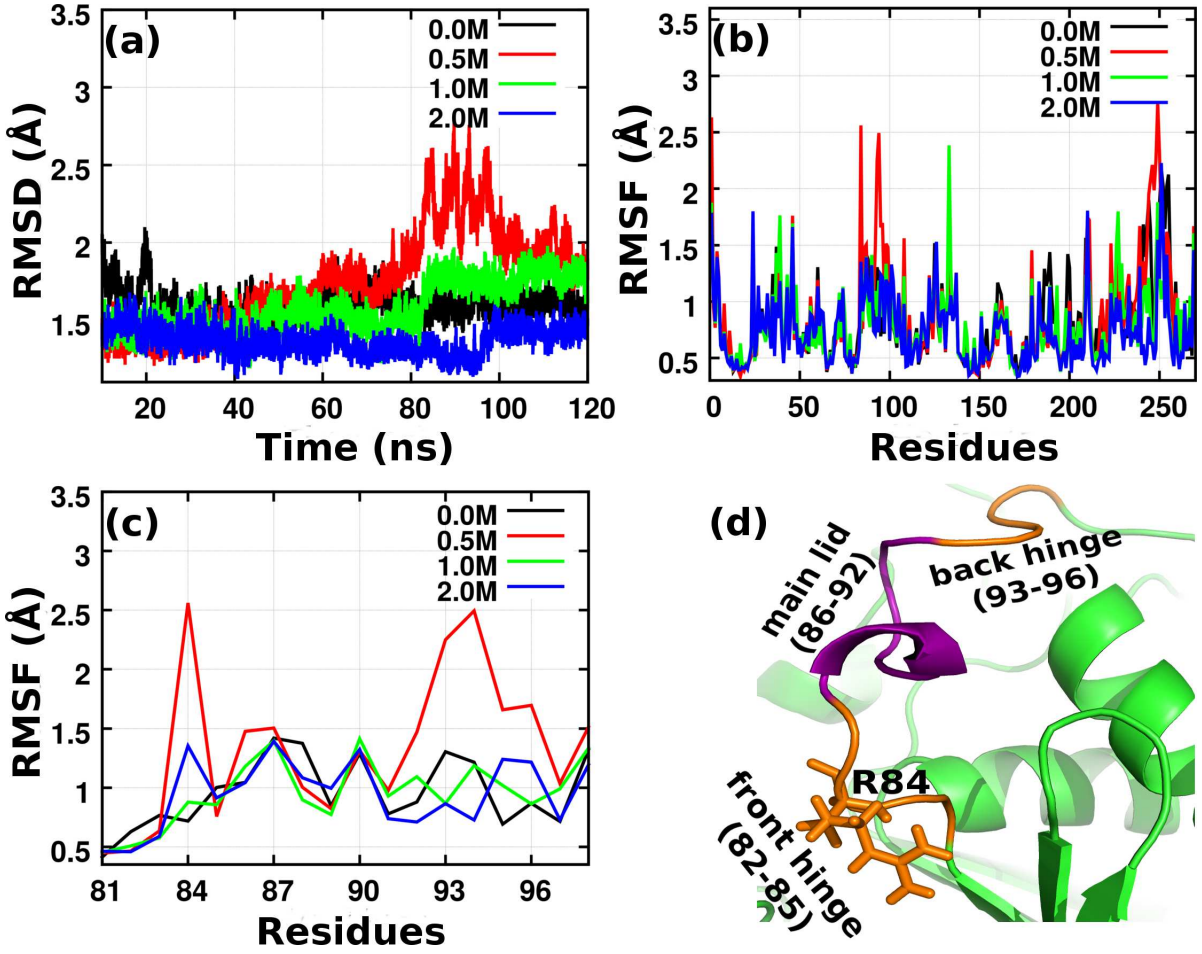

Figure 3: (a) RMSDs (averaged over all backbone atoms) as a function of simulation time and (b) RMSF (averaged over all atoms of each residue within 100-120 ns time interval) at all four IL concentrations in the open form of TLL with respect to the same form of the enzyme (energy minimized in pure water), (c) RMSF of lid residues (zoomed from panel (b)), and (d) Different sections of the lid shown for open_0.5IL system.

1.2. Radius of gyration

Results on radius of gyration (R_g) of the whole enzyme, the core regions and the lid are presented in SI (See "Radius of gyration (R_g)" in SI). These too support the observations made from RMSD and RMSF. In addition, these also agree with a common feature of interfacial activation, i.e., the surface hydrophobic residues get exposed more toward the solvent with decreasing solvent polarity,[8–10] and this effect is more prominent in the flexible lid region in open conformation.

1.3. Intra-protein and protein-solvent interactions

To understand the overall conformational changes of TLL in more detail, we have examined the changes in intra-protein as well as protein-solvent hydrogen bonding interactions with increasing IL concentration. The complete data is presented in Supporting Information (see "Intra-protein and protein-solvent interactions" in SI) and a summary is provided here. Nonpolar surface residues of lipases get more exposed to solvent whereas the side chain of polar surface residues get buried inside with decreasing solvent polarity. The number of lid-solvent hydrogen bonds is highest for the open_0.5IL system, making it more active for catalysis.

2. Changes in the active site

In the open form (fully activated)[23] of TLL, the hydroxyl oxygen atom (OG) of S146 from the trypsin-like catalytic triad (Figure 4 top), performs a nucleophilic attack on the carbonyl carbon of the lipid or ester substrate. The nucleophilicity of S146 hydroxyl oxygen (OG) is increased by the hydrogen bond formed between one of the imidazolium nitrogen (NE2) of H258 and the hydrogen attached to the nucleophilic oxygen (OG) of S146. Another imidazolium hydrogen attached to the nitrogen (ND1) of H258 forms two hydrogen bonds with two carboxyl oxygens (OD1 and OD2) of the third catalytic residue D201 which helps H258 to maintain the best orientation of the imidazolium plane for the formation of the

strongest possible hydrogen bond between histidine H258(NE2) and serine S146(hydrogen attached to OG). After the nucleophilic attack, a tetrahedral oxyanion intermediate is formed which is stabilized by the oxyanion hole formed by the backbone NH group of L147 and S83.[30]

From Figure 4(a), we observe that the catalytic hydrogen bond between NE2(H258) and hydrogen attached to OG(S146) is the strongest (3.0 Å) in 0.5M and 1.0M IL solvents. Though the OD1(D201)-ND1(H258) hydrogen bonding distance is the shortest (2.75 Å) in the 2.0M IL solvent (Figure 4(b)), OD2(D201)-ND1(H258) hydrogen bonding distance is the strongest (2.65 Å) in all the systems except in open_2.0IL (Figure 4(c)). Again, in the open_0.5IL system, residue S83 forming oxyanion hole remains at the largest distance apart from the catalytic residue S146 (Figure 4(d): OG(S146)-N(S83) distance is 8.6 Å) compared to other systems. This leads to an easier nucleophilic attack by OG(S146) on the substrate which can approach closer to the catalytic triad without any hindrance from S83. Thus, the catalytic triad of TLL becomes most active for nucleophilic attack on the substrate followed by stabilization of the tetrahedral intermediate by the oxyanion hole in the 0.5M IL solvent. In the closed form too, the closed_0.5IL system is found to have one of the most effective active site for catalysis (Figure S13), following similar arguments.

3. W89 flip: optimal substrate binding rate

Tryptophan (W), being one of the amino acids forming the aromatic belt in the transmembrane segment of membrane protein,[89] is one of the best candidates to interact with the lipid surface due to the amphiphilic nature of its side chain. So, in the presence of lipid or an ester substrate, the lid residue W89 stays over the substrate bound to the active site and influences the process of substrate binding to the enzyme at an optimal binding rate.[21,90]

3.1. Three different orientations for W89

W89 can give rise to optimal substrate binding rate only when its side chain is oriented exactly above the substrate, if not, at least within the active site pocket. However, it is not

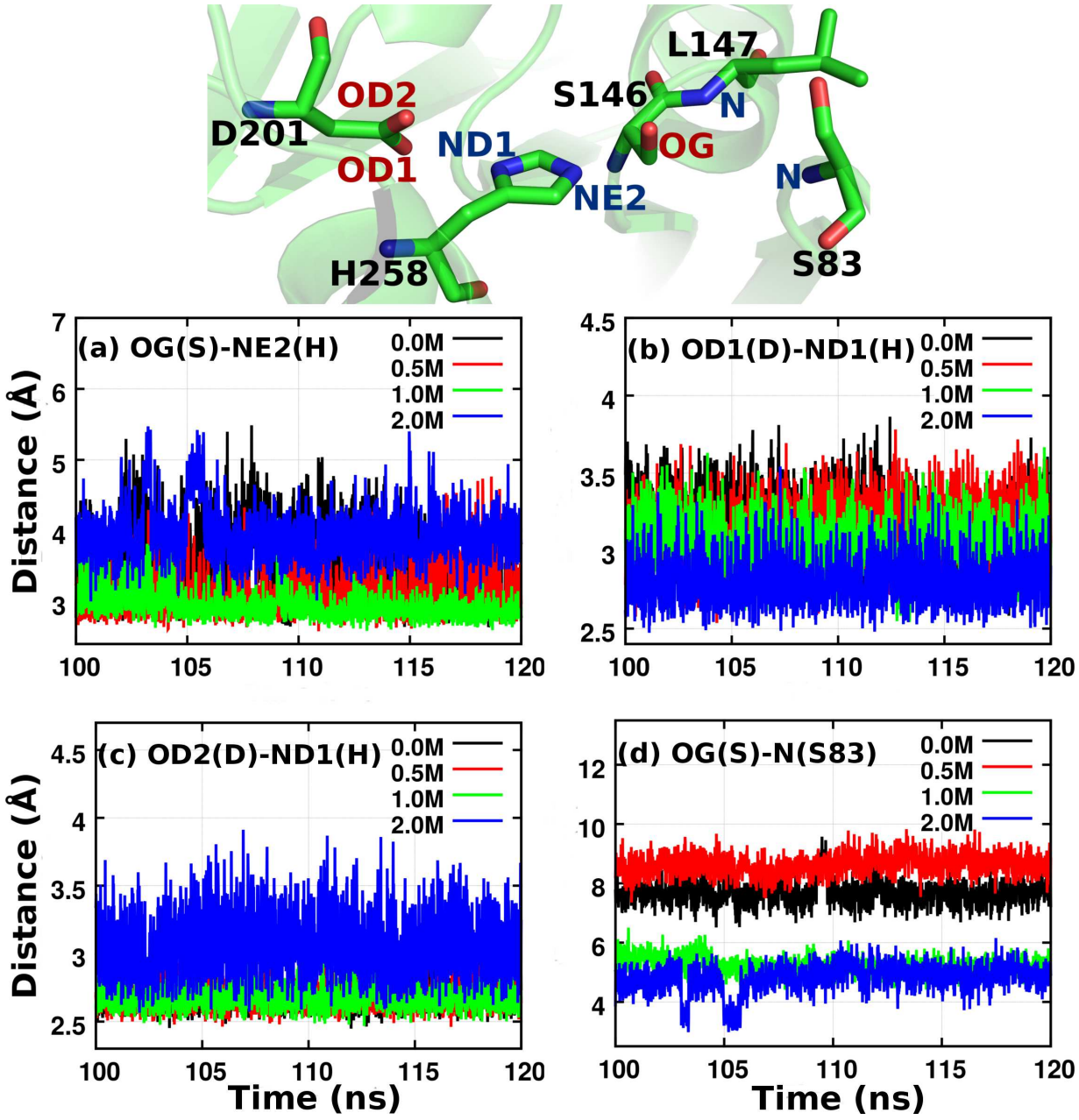

Figure 4: **Top:** Catalytic triad (D201-H258-S146) and oxyanion hole (L147-S83) of the active site for TLL in open crystal structure (1DTE). Color scheme: oxygen (red), nitrogen (blue) and carbon (light green). Hydrogens are not shown for clarity. **Bottom:** Donor-acceptor distance of hydrogen bonding interactions for all the four systems in the open form of TLL: (a) OG(S146)-NE2(H258); (b) OD1(D201)-ND1(H258); (c) OD2(D201)-ND1(H258); (d) OG(S146)-N(S83). Donor-acceptor (D-A) pairs whose distance is less than 3 Å and H-D-A angle is less than 30^0 are considered here as hydrogen bond.

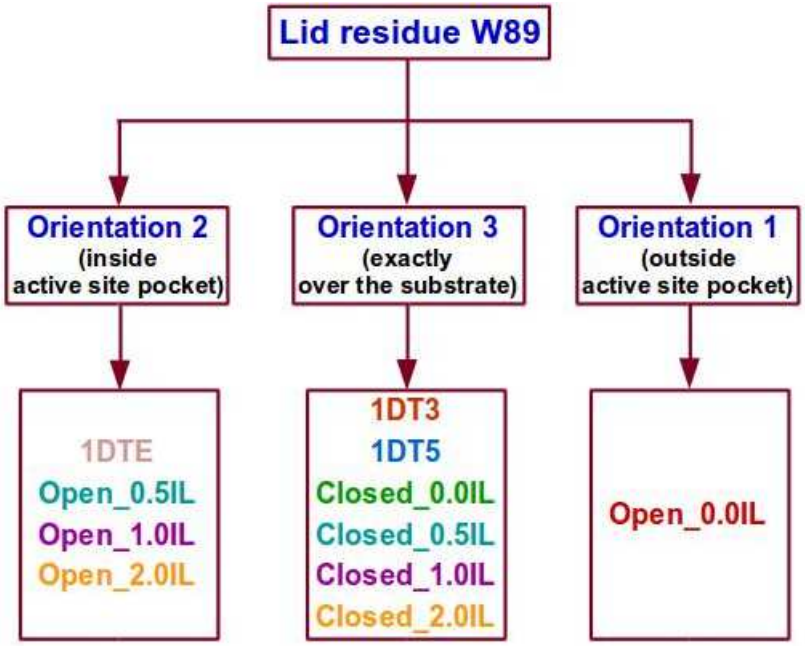

Figure 5: Classification of the systems with respect to the side chain orientation of W89. 1DT3, 1DT5 and 1DTE are low activity closed, activated closed and fully activated open crystal structures of TLL, respectively.

always possible to achieve this orientation. W89 shows three possible orientations depending on the open-closed conformation of the lid, as well as on the presence or absence of IL or surfactant in the solution (Figures 5 and 6(a)). In the apo form (enzyme, without any bound ligand) of the open enzyme in pure water (system open_0.0IL containing 1DTE), the side chain of W89 is oriented away from the active site and is located within a hydrophobic microenvironment[21] formed by the side chain of nearby residues I86, I90, F113, L147 and L206 (Figure 6(b): **orientation 1**). On the other hand, due to the presence of surfactant during the time of crystallization of TLL in the open state (1DTE), W89 remains within the active site pocket (Figure 6(c): **orientation 2**). Such an orientation can aid the easy exposure of W89 toward solvent on increasing surfactant concentration. However, this kind of exposure would not be so easy if W89 orients toward the congested hydrophobic microenvironment and away from the active site. And this is also true for the open TLL solvated in aqueous IL solution (i.e., open_0.5IL, open_1.0IL and open_2.0IL systems) and as a result, in these systems too, W89 remains in **orientation 2** (Figure 6(c)). (Although

both IL and surfactant play essentially the same role, the rationalization of our choice of IL over surfactant is discussed in "Rationalization of the choice of IL over surfactant" in SI.)

In *all the closed systems,* independent of IL concentration, the lid is locked to the closed state due to the hydrophobic interaction with a nearby random loop (residues 202-211) (Figures S3 and S4). This rigidity of the lid makes lid residue W89 to be fixed exactly over S146 and the oxyanion hole (i.e., exactly over the position where the substrate is expected to bind) in all the closed systems as well as in the closed crystal structures (1DT3 and 1DT5) (Figure 6(d): **orientation 3**).

3.2. IL concentration dependent flipping of W89

Although the simulation of the open form (open_0.0IL) was initiated from 1DTE in which W89 is oriented toward the active site pocket (Figure 6(c): W89 in wheat color, having orientation 2), it soon flips back (at ∼17 ns simulation time frame) into the hydrophobic microenvironment (Figures 6 (b) and (c): W89 in red color, having orientation 1), due to the absence of surfactants and IL. By the same analogy, the addition of IL to result in the open_0.5IL system causes W89 to flip from the microenvironment toward the active site pocket (Figure 6(c)). This W89 flip in the open_0.5IL system is rationalized in further detail below.

As discussed earlier, in the presence of IL, hydrophobic interactions within the enzyme decrease, and the surface hydrophobic residues get more exposed to the less polar solvent.[19,23] This fact is also evident from the increase in R_g of the lid in the open form of TLL upon increasing IL concentration (Figure S8(d)). Thus, with the increase of IL concentration, exposure of protein surface hydrophobic residues I86, I90 and L206 toward the solvent weakens the hydrophobic interaction of residue W89 with the surrounding hydrophobic microenvironment[91] (Figure 6(b)). Due to the presence of an amphiphilic side chain, W89 too would prefer to be exposed toward the aqueous IL solvent. However, this process is hindered by the congested hydrophobic microenvironment and the nearby D57-D62 hinge

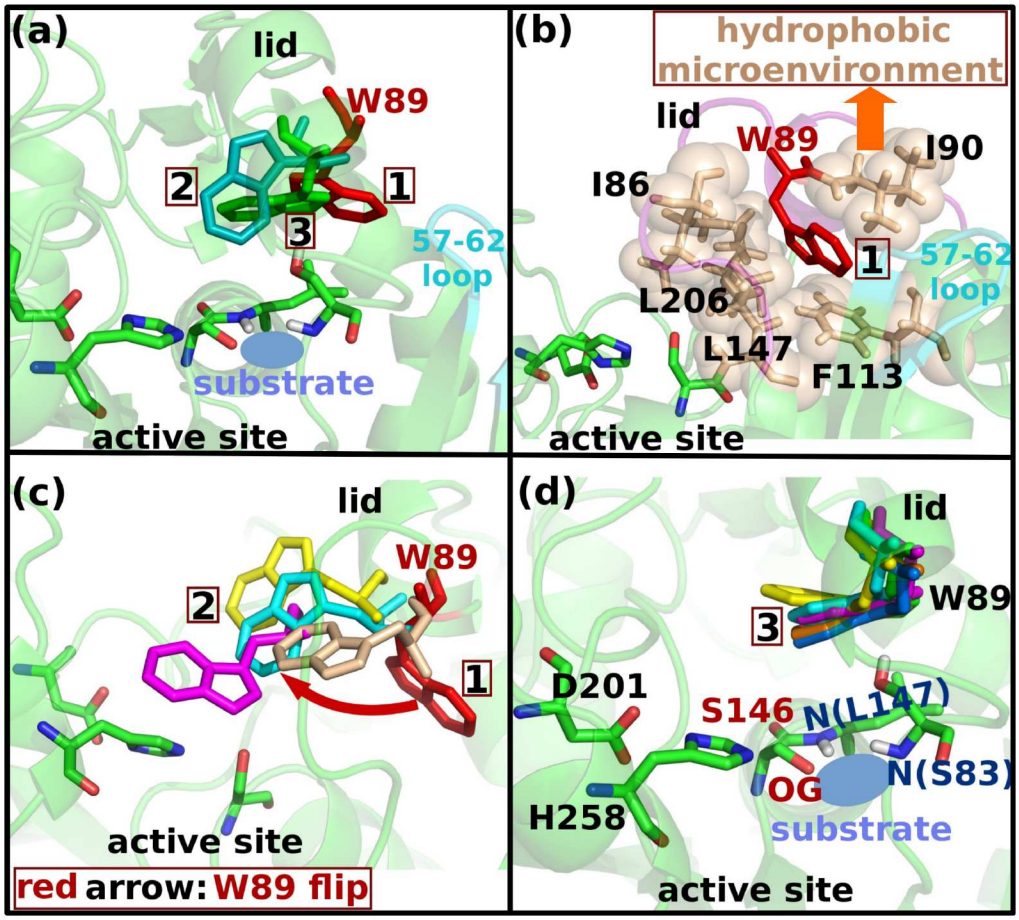

Figure 6: **Three different orientations of W89.** Simulation structures are taken from the last frame of the 120 ns trajectories of each system. Overall protein and the active site residues are shown for the closed_0.0IL system (panel (a) and (d)) and the open_0.0IL system (panel (b) and (c)). Sky blue colored ellipse represents the expected substrate binding position. Hydrogen atoms of active site residues and W89 are not shown for clarity except for residues S83 and L147 where only polar hydrogen atoms are shown. (a) **Three different orientations of W89.** **1**: W89 within hydrophobic microenvironment, i.e., outside the active site pocket in open_0.0IL system (W89 shown in red). **2**: W89 within active site pocket in open_0.5IL system (W89 shown in cyan). **3**: W89 exactly over the substrate binding position in closed_0.0IL system (W89 shown in light green). (b) **Orientation 1**: Residues forming hydrophobic microenvironment (in open_0.0IL system) are represented in sticks as well as sphere with wheat color. For clarity, the lid is shown in transparent purple. (c) *W89 flipping* from open_0.0IL (red) to open_0.5IL (cyan) system. All the systems having W89 in **orientation 2** (1DTE: wheat, open_0.5IL: cyan, open_1.0IL: magenta and open_2.0IL: yellow) are shown here. (d) W89 orients itself exactly over the substrate binding position (**orientation 3**) in all closed systems (0.0M: light green, 0.5M: cyan, 1.0M: magenta, 2.0M: yellow) and the closed crystal structures (1DT3: orange and 1DT5: marine).

(Figure 6(b)). Thus, in the presence of IL, instead of orienting outward, W89 prefers to flip into the active site cavity (which is somewhat less congested) by breaking its weaker hydrophobic interactions with that microenvironment (Figure 6(c)).

At lower IL concentration (0.5M), W89 points toward the active site; whereas at 1.0M concentration, it gets closer to the active site (Figure 6(c)). This observation is in contrast to the general expectation that the protein surface hydrophobic residues will get more exposed to the solvent on increasing IL concentration.

In this context, we have identified the existence of an intra-lid hydrogen bond between donor N88(ND2) and acceptor N92(OD1) with an average distance of 2.9 Å, in the case of open_1.0IL system (Figure 7 (c)). The formation of this H-bond is a consequence of the drastic decrease (from 37 to 30) in the number of lid-solvent hydrogen bonds (Figure S11(d)), on increasing the IL concentration from 0.5M to 1.0M. It should be noted, however, that the formation of this intra-lid hydrogen bond converts the lid from a 3_{10}-helix (for 0.5M) to an almost α-helix or a random coil (for 1.0M) (Figure 7 (b) and (c) respectively). This change in the lid helicity makes R84 and W89 in the open_1.0IL system to come closer to the D57-D62 region (Figure S16) and the catalytic triad (Figure 6(c)), respectively. However, on further increase to 2.0M concentration of IL, N92 breaks the hydrogen bond with N88 and forms a new hydrogen bond with H110 with an average distance of 2.9 Å between the acceptor N92(O) and donor H110(NE2) (Figure 7 (d)). As a result, the lid changes from a nearly α-helix or a random coil (for 1.0M) to a perfect α-helix (for 2.0M) (Figure 7 (c) and (d) respectively), which in turn makes W89 get exposed to the solvent to an extent greater than that seen in the open_0.5IL system (Figure 6(c)). This change in lid helicity with increasing IL concentration is concomitant with the exposure of lid residue N92 moving away from the active site and getting exposed to the solvent (Figure S14).

Although W89 moves closer to the active site in the open_1.0IL system (than at 0.5M IL concentration), it orients itself on the approach path of the substrate to S146 (Figure 6(c)); as a consequence, substrate binding to the active site (where S146 is located) is sterically

hindered. On increasing IL concentration further to 2.0M, W89 moves away from the active site, as expected. Thus, *among all the open systems, it is only at 0.5M concentration that W89 stays near the substrate binding position, but does not orient itself too closer to the active site to hinder the substrate binding process.* (Figure 6 (c) and (a), respectively; W89 shown in cyan color for open_0.5IL). Again, in the closed_0.5IL system, W89 remains exactly above the substrate binding position (Figure 6(d)) like in all other closed systems. So, in terms of W89 orientation too, the 0.5M system is most effective for optimal substrate binding rate.

4. W89 flip triggers Arginine (R84) switch

The W89 flip is one of the major guiding forces behind the arginine (R84) switch which constitutes the primary event in the interfacial activation of TLL. As discussed earlier, R84 switch distinguishes the low activity, closed form (1DT3) from the activated, closed form (1DT5) of TLL. Thus, the observation of the W89 flip in the simulations of the fully activated, open form of the enzyme in the presence of IL is significant and portends to a subsequent R84 switch, which we shall now examine.

On increasing the IL concentration from 0.0M to 0.5M (from Figure 7 (a) to 7 (b)), the flip of W89 toward the active site converts the residues 86-89 of the lid from a random loop to a short 3_{10}-helix by dragging residue N88 closer to G61 of nearby D57-D62 loop hinge. As a result, the residues 82-88 region gets closer to D57-D62 hinge via weak electrostatic interactions between S83, N88, G61 and D62 (Figure 7 (b)). These observations are supported by the positive correlation in the dynamical cross correlation maps (DCCM) between residues 82-88 and residues 57-62 loop in the presence of IL (positive correlation between these two loops had also been found by Gunasekaran *et al.*[29]), whereas these two regions are almost uncorrelated in pure water (Figures S15 and S1) wherein the lid has a random loop configuration (Figure 7 (a)). The formation of intra-lid hydrogen bond between N88(hydrogen attached to ND2) and N92(OD1) (for 1.0M) followed by intra-protein hydrogen bond N92(O)-H110(hydroge

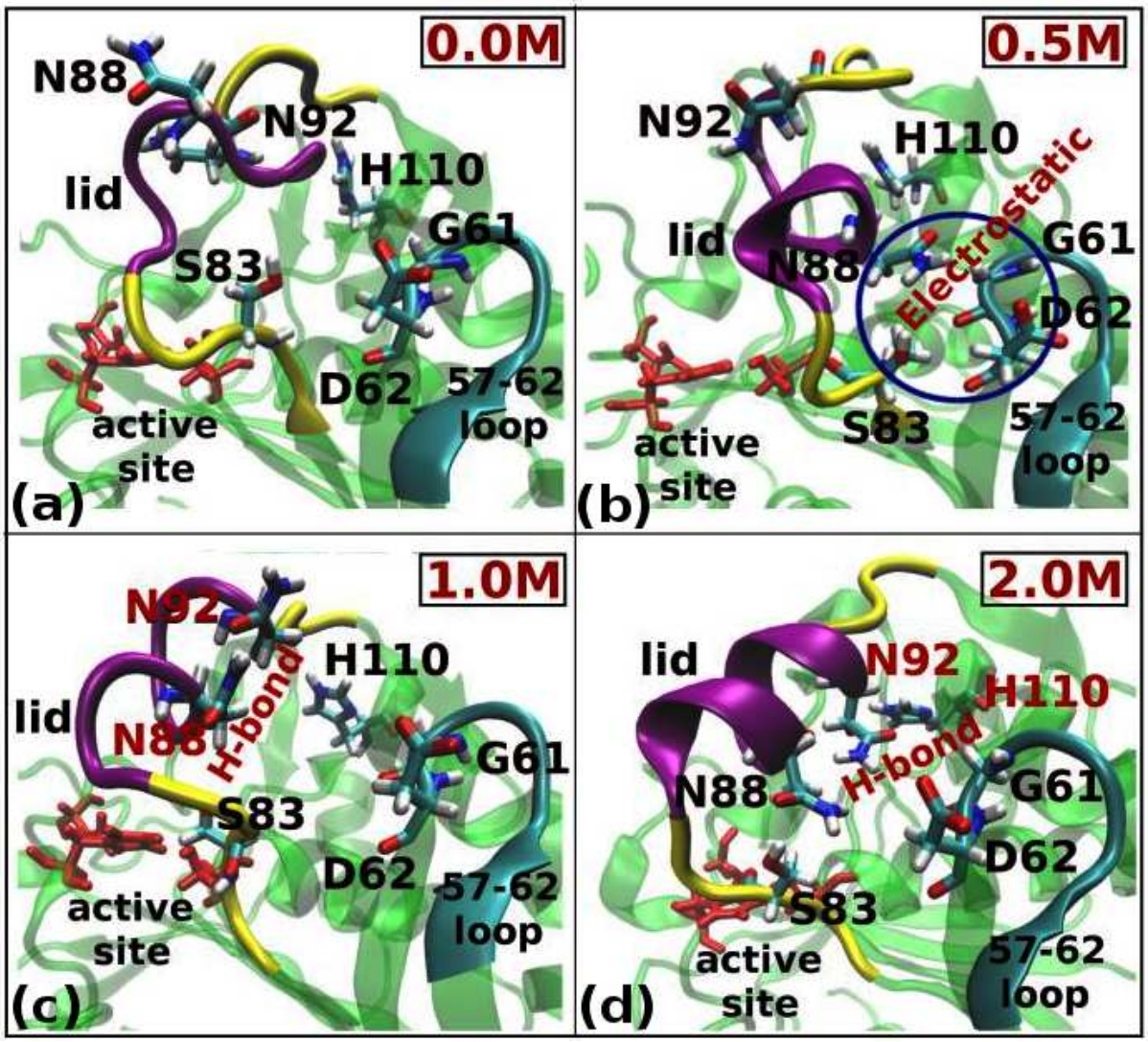

Figure 7: Lid helicity, and correlation between the lid and 57-62 loop in the last frame: Lid, its front and back hinges, and 57-62 loop are displayed in purple, yellow, and cyan respectively. Residues forming hydrogen bonds between them are labeled with red letters. In the 0.5M system (b), residues within the blue circle (G61, D62, S83 and N88) interact electrostatically which result in a positive correlation between the lid and 57-62 loop in DCCM (Figure S15). The essence of the present figure can easily be captured from the change in helicity as well as position of the lid (shown in magenta color) on going from 0.0M to 2.0M.

attached to NE2) (for 2.0M) weakens the electrostatic interactions between the lid and D57-D62 loop (Figure 7 (c) and (d) respectively). Thus, with the increase in IL concentration from 0.5M to 2.0M, residues 82-88 move away from the 57-62 loop (DCCM plot shows reasonably good correlation to anticorrelation, on changing IL concentration from 0.5M to 2.0M). These events support the observation of the conversion of the lid (especially residues 86-89) from a 3_{10}-helix (for 0.5M) to an almost α-helix or a random coil (for 1.0M) followed by a perfect α-helix (for 2.0M) (Figure 7 (b), (c) and (d) respectively). Due to the positive correlation in DCCM between 82-88 and 57-62 regions for the 0.5M system, R84 switches (Figure 8 and S16) from G266-C268 to D57 zone by forming a hydrogen bond with D57 (just before the switch, i.e. at around 106 ns, the average distances of R84(CA) from G266(O), C268(O) and D57(CG) are 9.7, 10.7 and 8.7 Å, respectively). In summary, we have observed that W89 flip induces a change in lid helicity in such a way that R84 gets trapped around C268, D57-D62, and G266-C268 for 0.0M, 1.0M and 2.0M systems, respectively whereas it switches over all these regions in only 0.5M system (Figure 8 and S16). In the course of interfacial activation of TLL, a similar arginine (R84) switch, on going from low activity (LA) form to activated (A) form of TLL had been demonstrated by Brzozowski *et al.*[23] through a crystallographic study (Figure 2 top).

In the closed forms of the enzyme, due to the absence of W89 flipping (Figure 6(d)), the extent of R84 switch is reduced, and it is only observed in the closed_1.0IL system and is fully absent in the closed_0.5IL system (Figures S6 and S7). From the comparison between the open and closed system in 1.0M IL concentration, it is observed that instead of coming closer to the random loop (residues 202-211), the lid goes far from that loop in the closed lid conformation (Figure S3). As a result, the hydrophobic interactions between the lid and that loop become least favorable, which may be the cause for R84 switch in the closed_1.0IL system.

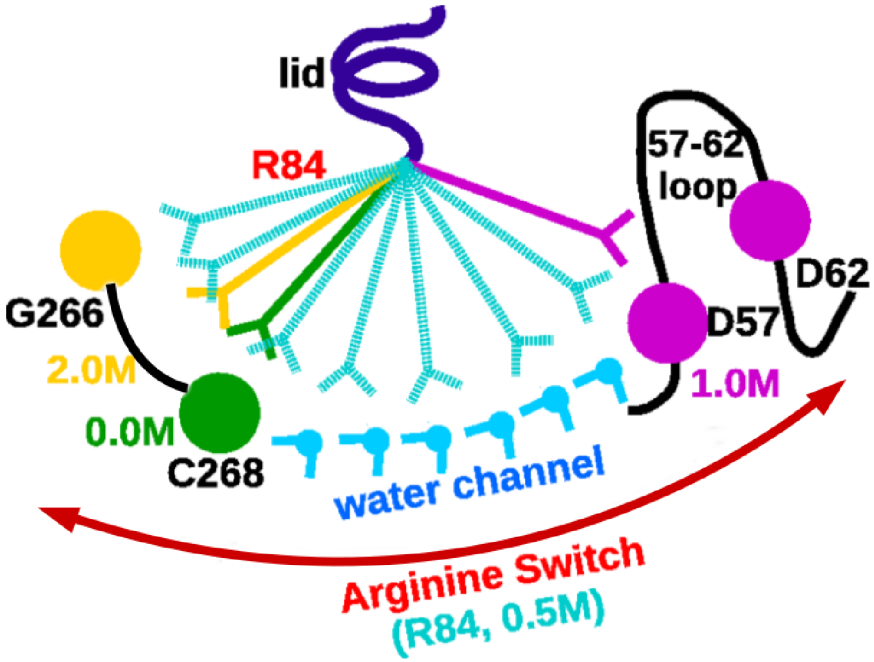

Figure 8: Schematic of arginine (R84) switch through water channel in the open_0.5IL system. For detailed description directly from simulation trajectories, see Figures S16, S17, S18 and S19.

5. Arginine (R84) switch through water channel

5.1. Water-structure breaking vs. direct water-protein interactions

The R84 switch is caused not only by the IL concentration dependent flip of W89, but is also mediated by the water molecules surrounding the enzyme. In general, the addition of IL in the solvent results in the rupture of the micro-aqueous phase[92] surrounding the enzyme, leading to the destabilization of the native fold of the protein.[42,50–52,54,55] However, in the analyses of R_g of the overall protein (Figures S8(c) and S10(c)), and of intra-protein as well as protein-solvent H-bonding (Figures S11(a), S11(b), S12(a) and S12(b)), ILs are found to additionally stabilize the protein, indicating that the disruption of water network plays only a minor role. This observation is in line with the experimental outcome that water-structure plays a secondary role in stabilizing the protein.[42,93] We can now assume two scenarios: in the first, water molecules surrounding the enzyme in the 0.0M system are reluctant to interact with the protein surface residues, due to the stronger water-water hydrogen bonding

than that between water and protein. Secondly, in systems with ILs, few water molecules in the thin water layer get replaced by cations or anions of ILs. This replacement *weakens the extended hydrogen bonding network in water* (secondary factor)[42,93] that makes the *direct water-protein interactions* (primary factor) more probable.

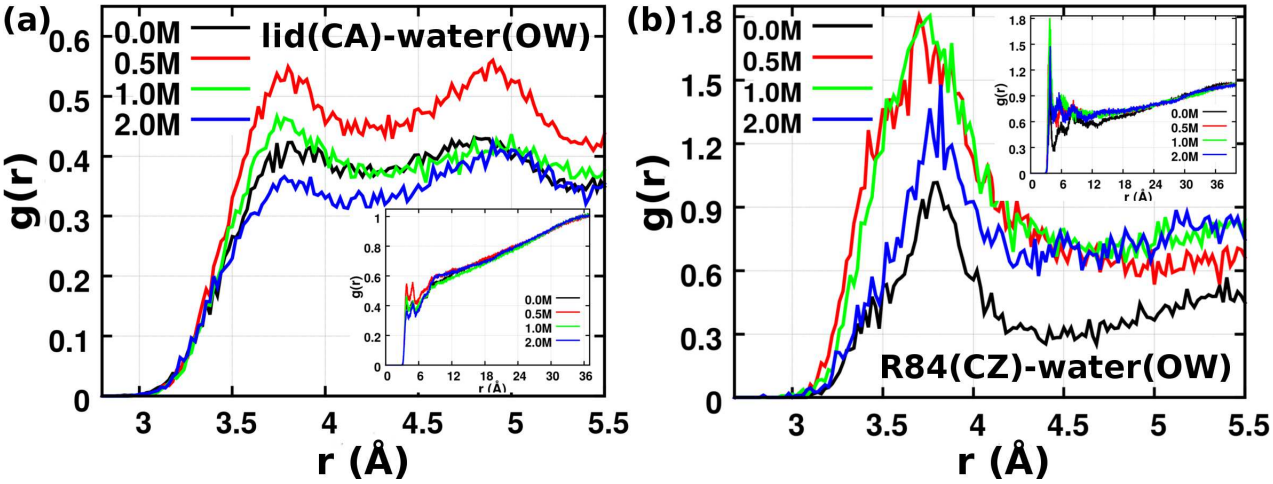

Figure 9: Radial distribution function (RDF) g(r) for C_α-atom (CA) of lid residues (a) as well as for carbon atom CZ at the terminal group of the side chain of R84 (b) with the oxygen atom (OW) of water for all four systems containing TLL in open form in the 100-120 ns time window. RDF plots are shown only up to first or second coordination shell of the corresponding atom whereas the whole RDF plots are shown in the inset.

Table 1: Coordination number (CN) of solvent with respect to all lid residues as well as with respect to R84 obtained from the 100-120 ns time window of MD simulations of TLL in its open form.[a]

RDF pair	Solvent concentration (M)	CN in first coordination shell
CZ(R84)-OW	0.0	4.2
	0.5	**8.8**
	1.0	8.1
	2.0	4.9
CA(lid)-OW	0.0	2.1
	0.5	**2.4**
	1.0	1.9
	2.0	1.3
CZ(R84)-C(GLS)	0.5	0.1
	1.0	0.2
	2.0	1.8
CZ(R84)-O(CHL)	0.5	0.2
	1.0	0.8
	2.0	1.9

[a]Values at 0.5M IL concentration are in bold to show the "optimal" values. CZ: carbon atom at the terminal group of side chain of R84; CA: α-carbon of all lid residues; OW:oxygen atom of water; C(GLS): carbonyl carbon atom of glycinate anion; O(CHL): hydroxyl oxygen atom of cholinium cation. A similar table (Table S3) showing the results for closed systems is provided in SI.

5.2. Existence of water channel: Arginine switch

To obtain a closer insight into the direct water-protein interactions, we have calculated the radial distribution functions separately for water, cholinium and glycinate with the lid residues as well as with R84 (Figures 9 ((a) and (b) respectively) and S20) and also the corresponding coordination numbers (CN) (Tables 1 and S3). In all the systems, the lid residues are mainly solvated by water along with a few IL ions (mostly cholinium, due to its chaotropic nature[94,95]) in the first coordination shell. With increasing IL concentration (from 0.5M to 2.0M), more water molecules in the water layer surrounding the protein are replaced by IL ions, leading to the decrease in water CN of lid residues, including of R84 (Table 1). However, with the increase of IL concentration from 0.0M to 0.5M, a water channel between

C268 zone to D57 zone is formed by the water molecules that are somewhat freed from the water-structure which is weakened in the presence of IL (Figure S17). Consequently, *R84 in the open form of TLL easily switches back and forth (in the 60 to 110 ns simulation time window) between the G266-C268 and the D57 zones through the flexible water channel by making and breaking consecutive hydrogen bonds with the water molecules* (Figures 8, S16, S17 and S18). Thus, this water channel mechanism for the R84 switch is an example of direct water-protein interaction as a consequence of water-structure weakening in the presence of IL. However, the back and forth arginine (R84) switch was also observed multiple times when the trajectory of the open_0.5IL system was extended up to 300 ns (Figure S19 and "**Arginine switch movie**" in SI). Due to this switch, the lid residue R84 covers a large surface area of accessible solvent which leads to higher CN of water with respect to both lid residues (CA atom) and R84 (CZ atom) in the open_0.5IL system compared to that in the open_0.0IL system (Table 1). A further increase in IL concentration increases the CN of less mobile IL ions with respect to R84 by replacing some more mobile water molecules both from the water channel and G266-C268 and D57-D62 zones (Table 1). The fewer number of water molecules around R84(CZ) in open_0.0IL and open_2.0IL systems (CNs are 4.2 and 4.9, respectively) preclude the formation of such a water channel which makes R84 switching forbidding. As a result, R84 becomes locked within particular zones at both 0.0M (C268 zone) and 2.0M IL (G266-C268 zone) concentrations (Figure 8, S16, S17 and S18). However, in the open_1.0IL system, the CN of water around R84(CZ) is close to that in the open_0.5IL system (CNs are 8.1 and 8.8 respectively). So, on increasing IL concentration from 0.0M to 1.0M, R84 once switches from C268 to D57-D62 zones ($\sim$46 ns simulation time frame), but due to the formation of incomplete water channel (as CN is slightly lesser than that in 0.5M system) (see Table 1 and Figure S17), R84 cannot come back to the C268 zone; it becomes locked to D57-D62 zone (Figures 8, S16, S17 and S18). Thus, in the case of the open form of TLL, R84 switch is only possible for the system with IL concentration around 0.5M. This is also consistent with the very high value of RMSF of R84 in the open_0.5IL system (Figure

3(c)).

In the closed form, on the other hand, the first RDF peaks are of least height at 0.5M IL concentration (Figure S20). As a consequence, a sudden decrease in the CN of water with respect to CZ atom of R84 (as well as CA atom of the lid residues) is observed ongoing from the closed_0.0IL system to the closed_0.5IL one (Table S3). This supports the fact that R84 is locked to residue C268 in the closed_0.5IL system (Figures S6 and S7). Starting from the open crystal structure (1DTE), the lid in open_0.5IL system moves toward closed conformation, but it does not reach to the closed state, rather it remains in between open and closed lid conformation (actually more toward open conformation) (Figure S1). So it is not possible for the lid in closed_0.5IL system to come to the open state. This is also in line with the R84 orientation (locked to C268) in this system.

5.3. Solvent structure around 0.5M IL concentration

The results presented so far naturally leads to the following question: what makes the IL concentration around 0.5M so special? Is the solvent structure at IL concentration around 0.5M different from all others? We have examined this aspect on the basis of solvent-solvent radial distribution functions and results from these are discussed in "Solvent structure around 0.5M ChGly IL concentration" in SI. From this discussion, it is concluded that *no special solvent structure is seen around 0.5M IL concentration*. The speciality of this optimum concentration does not lie within the solvent structure (which is also a secondary factor for protein stabilization[42,93] as mentioned earlier), rather it lies within the primary factor, i.e., the direct water-protein interactions, which has been proved, from the analyses of coordination number, to be the best for IL concentration around 0.5M.

6. Interfacial activation: bridging theory and experiment

Interfacial activation of lipases needs a hydrophobic surface to which the lid hydrophobic residues can be attached.[50–52,54,55,96] This hydrophobic surface may either be formed by lipid

substrate or hydrophobic solvent (surfactant) in their aggregated form.[50,52,54,55] In the current study, however, cholinium cations and glycinate anions are seen to exist in monomeric form (Figures S23 and S24) at all concentrations. Furthermore, the present study does not include any substrate in the enzyme. Thus, in the present set of simulations, it is very tough for TLL to be interfacially activated without aid from any hydrophobic surface.

However, the radius of gyration and intra-protein and protein-solvent hydrogen bonding interactions demonstrate that with the increase in IL concentration, hydrophilic residues get buried away from the solvent, and the side chains of hydrophobic residues get exposed to the solvent. These are precisely the signatures of interfacial activation.[23] Considering these aspects, we can conclude that, *although both substrate and surfactant are absent in the present study, the presence of IL can lead to interfacial activation of TLL.* Furthermore, the presence of IL increases the ionic strength of the solvent compared to pure water, which in turn decreases the critical micellar concentration (CMC) of the lipid substrate (which is absent in our study, but will be present during catalysis), and hence enhance the rate of interfacial activation for systems containing IL compared to that in pure water.[97] Further investigations are required to confirm this hypothesis.

Furthermore, all the structural changes observed in TLL in the present study as a function of IL concentration (Tables S5 and S6) are comparable to the changes which are reported to happen during interfacial activation of TLL (i.e., the changes occur on going from 1DT3 to 1DT5 to 1DTE form of TLL as described by Brzozowski *et al.*[23]) (Figures 1 and 2). This comparison results in the conclusion that *disulfide isomerization and α_0-helix formation are just the initiation steps, but arginine (R84) switch (or R84 orientation) plays the most crucial role toward the interfacial activation of this lipase enzyme* (for detail, see "Arginine (R84) switch: the most crucial step toward interfacial activation" in SI). Thus, considering this aspect along with the lid conformation, it can be concluded that only for the open_0.5IL system, the features related to interfacial activation almost match with that of the fully activated (FA) form of TLL (Table S5). By the same analogy, TLL in closed_0.5IL system is

similar to the activated (A) form of TLL (Table S6). So, the conversion of TLL from closed to open form in 0.5M IL concentration can be considered to be similar to the conversion of A to FA form of TLL in the presence of lipid or surfactant, which is basically the last step of interfacial activation[23] (Figure 1). Based on the mechanism of interfacial activation, our computational observations thus rationalize the experimental result of 0.5M IL concentration being the optimal one for enzymatic activity.

7. A promising application in biodiesel production

The catalytic activity of TLL in the hydrolysis of *p*-nitrophenyl esters has been investigated earlier.[62] It is to be noted that the same type of substrates (ester or fatty acid) are also used for transesterification reactions involved in biodiesel production. As the current computational study does not involve any substrate, our findings can be applied to any ester or fatty acid substrate. Thus, our theoretical study along with the existing experimental findings can be useful for biodiesel production as well, wherein TLL is known to be one of the most popular enzyme.[4] Furthermore, the use of an optimum concentration of IL with TLL can not only enhance the biodiesel production rate, but also can avoid enzyme inactivation by acyl acceptors (generally alcohol solvent).[98] The same can yield production rates even higher than the solvent-free system which was earlier thought to be one of the best possible environment for biodiesel production against enzyme inactivation by acyl acceptors.[99,100]

Conclusions

In summary, we have observed that the addition of IL to water makes the open form of the enzyme compact, but makes the lid region less compact and more flexible. The enhanced interaction of the two lid proximal hinges (residues 82-85 and 93-96) with the solvent in the open_0.5IL system, enables rigid body hinge-type facile opening and closing of the lid.[22,88] Furthermore, the active site catalytic triad for this open_0.5IL system is most effective and

opened up to substrate. The presence of IL at 0.5M concentration with the open form of TLL helps lid residue W89 to flip into the active site pocket, whereas in the closed form, it orients itself exactly over the substrate binding position that can contribute to substrate binding process.[21,90] The W89 flip from a hydrophobic microenvironment (in pure water, apo form) into the active site pocket (at 0.5M IL concentration) can be experimentally verified using tryptophan fluorescence.[25,101] This W89 flip triggers the arginine (R84) switch which is related to the well-known interfacial activation of TLL.[23] Furthermore, the 0.5M IL solution is found to be optimal for creating a dynamic water channel between two regions (C268 and D57) which leads to facile R84 switching between them. *In the solution containing 0.5M IL with the open form of TLL, the enzyme attains a structure that is closest to its fully activated (FA) form.*

Furthermore, the closed form of TLL is most stable in this 0.5M IL concentration only. In it, the R84 residue is locked with C268, which makes the TLL structure resemble the activated (A) form. Thus, the closed to open conversion of TLL at only 0.5M IL concentration becomes similar to the conversion of TLL from the A to FA form which happens in the last step of interfacial activation of TLL (Figure 1).[23] This makes TLL be catalytically most potent at 0.5M IL concentration. Thus, almost all of our theoretical observations, correlating the interfacial activation of TLL, agree with the recent experimental observation[62] of catalytic rate to be optimal at 0.5M IL concentration.

Needless to state, the simulations of the enzyme in aqueous IL solutions have been performed only at few IL concentrations. Thus, the simulation results, which show 0.5M IL concentration to be optimal for processes related to interfacial activation, should be qualified with this caveat. Identifying the exact concentration at which such interfacial activation processes are robust is beyond the scope of the present study.

Our investigation shows that the presence of IL with an optimum concentration can lead to the interfacial activation, even in the absence of any substrate or surfactant. Thus, the enzyme does not have to be activated again to uptake the substrate, which in turn enhances

the overall catalytic rate.

It has also been found that the SG268-SG22 disulfide isomerization and formation of an α_0-helix in the chain containing residues 23-28 are just the initiation steps, but arginine (R84) switch is the most important step toward interfacial activation of TLL. Thus, the present study not only proposes a reasonable molecular mechanism behind this optimum IL concentration dependent activity of TLL, but also provides a microscopic insight into interfacial activation mechanism of this enzyme. Moreover, the lid flexibility through water channel, being the most crucial step of interfacial activation, is general enough to explain the molecular mechanism behind the optimum solvent concentration dependent enzymatic activity of not only TLL enzyme, but also all lipases involving interfacial activation. *Based on this generalization of the basic concept*, we can search for the best possible combination of lipase and solvent with optimum solvent concentration which can open up a broad scope of application of enzymes in protein engineering and catalysis in a diverse area starting from the food industry to biodiesel production in an eco-friendly manner.

ASSOCIATED CONTENT

Supporting Information

System preparation, force field parameterization for ChGly IL, lid conformations, RMSD (for closed TLL) and RMSF, hydrophobic interactions between residues 202-211 and the lid, radius of gyration, intra-protein and protein-solvent interactions, catalytic hydrogen bonds (for closed TLL), rationalization of the choice of IL over surfactant, exposure of the lid residue N92, DCCM, R84 orientations and its switch through water channel, RDF for lid and R84 with water (for closed systems) and corresponding CN, the solvent structure around 0.5M ChGly IL concentration, why cholinium and glycinate exist as monomers, Arginine (R84) switch: the most crucial step toward interfacial activation, Arginine (R84) switch movie. This material is available free of charge via the Internet at http://pubs.acs.org.

AUTHOR INFORMATION

Corresponding Author

*bala@jncasr.ac.in

+9180 22082808

Notes

The authors declare no competing financial interest.

ACKNOWLEDGEMENT

We acknowledge the Department of Science and Technology, India for support. SB thanks Sheikh Saqr Laboratory for a senior fellowship. SD acknowledges Council of Scientific and Industrial Research for partial financial support. SD thanks Anirban Mondal for his kind help in calculating DDEC/c3 charges.

References

(1) Ma, F.; Hanna, M. A. Biodiesel production: a review. *Bioresour. Technol.* **1999**, *70*, 1–15.

(2) Ruzich, N. I.; Bassi, A. S. Investigation of lipase-catalyzed biodiesel production using ionic liquid [BMIM][PF_6] as a co-solvent in 500 mL jacketed conical and shake flask reactors using triolein or waste canola oil as substrates. *Energy & Fuels* **2010**, *24*, 3214–3222.

(3) Bose, S.; Armstrong, D. W.; Petrich, J. W. Enzyme-catalyzed hydrolysis of cellulose in ionic liquids: a green approach toward the production of biofuels. *J. Phys. Chem. B* **2010**, *114*, 8221–8227.

(4) Fernandez-Lafuente, R. Lipase from Thermomyces lanuginosus: uses and prospects as an industrial biocatalyst. *J. Mol. Catal. B: Enzym.* **2010**, *62*, 197–212.

(5) Lotti, M.; Pleiss, J.; Valero, F.; Ferrer, P. Effects of methanol on lipases: Molecular, kinetic and process issues in the production of biodiesel. *Biotechnol. J.* **2015**, *10*, 22–30.

(6) Nielsen, P. M.; Brask, J.; Fjerbaek, L. Enzymatic biodiesel production: technical and economical considerations. *Eur. J. Lipid Sci. Technol.* **2008**, *110*, 692–700.

(7) Fukuda, H.; Hama, S.; Tamalampudi, S.; Noda, H. Whole-cell biocatalysts for biodiesel fuel production. *Trends Biotechnol.* **2008**, *26*, 668–673.

(8) Brzozowski, A.; Derewenda, U.; Derewenda, Z.; Dodson, G.; Lawson, D.; Turkenburg, J.; Bjorkling, F.; Huge-Jensen, B.; Patkar, S.; Thim, L. A model for interfacial activation in lipases from the structure of a fungal lipase-inhibitor complex. *Nature* **1991**, *351*, 491–494.

(9) Derewenda, Z. S. Structure and function of lipases. *Adv. Protein Chem.* **1994**, *45*, 1–52.

(10) Schmid, R. D.; Verger, R. Lipases: interfacial enzymes with attractive applications. *Angew. Chem. Int. Ed.* **1998**, *37*, 1608–1633.

(11) Mogensen, J. E.; Sehgal, P.; Otzen, D. E. Activation, inhibition, and destabilization of Thermomyces lanuginosus lipase by detergents. *Biochemistry* **2005**, *44*, 1719–1730.

(12) Fernandes, M.; Krieger, N.; Baron, A.; Zamora, P.; Ramos, L.; Mitchell, D. Hydrolysis and synthesis reactions catalysed by Thermomyces lanuginosa lipase in the AOT/Isooctane reversed micellar system. *J. Mol. Catal. B: Enzym.* **2004**, *30*, 43–49.

(13) Rodrigues, R. C.; Godoy, C. A.; Volpato, G.; Ayub, M. A.; Fernandez-Lafuente, R.; Guisan, J. M. Immobilization–stabilization of the lipase from Thermomyces lanuginosus: critical role of chemical amination. *Process Biochemistry* **2009**, *44*, 963–968.

(14) Cesarini, S.; Diaz, P.; Nielsen, P. M. Exploring a new, soluble lipase for FAMEs production in water-containing systems using crude soybean oil as a feedstock. *Process Biochemistry* **2013**, *48*, 484–487.

(15) Price, J.; Nordblad, M.; Woodley, J. M.; Huusom, J. K. Fed-batch feeding strategies for enzymatic biodiesel production. *IFAC Proceedings Volumes* **2014**, *47*, 6204–6209.

(16) Cesarini, S.; Haller, R. F.; Diaz, P.; Nielsen, P. M. Combining phospholipases and a liquid lipase for one-step biodiesel production using crude oils. *Biotechnology for biofuels* **2014**, *7*, 1.

(17) Price, J.; Hofmann, B.; Silva, V. T.; Nordblad, M.; Woodley, J. M.; Huusom, J. K. Mechanistic modeling of Biodiesel production using a liquid lipase Formulation. *Biotechnol. Prog.* **2014**, *30*, 1277–1290.

(18) Skjold-Jørgensen, J.; Vind, J.; Svendsen, A.; Bjerrum, M. J. Altering the activation mechanism in Thermomyces lanuginosus lipase. *Biochemistry* **2014**, *53*, 4152–4160.

(19) Tong, X.; Busk, P. K.; Lange, L.; Pang, J. New insights into the molecular mechanism of methanol-induced inactivation of Thermomyces lanuginosus lipase: a molecular dynamics simulation study. *Mol. Simul.* **2016**, *42*, 434–445.

(20) Jutila, A.; Zhu, K.; Tuominen, E. K.; Kinnunen, P. K. Fluorescence spectroscopic characterization of Humicola lanuginosa lipase dissolved in its substrate. *Biochimica et Biophysica Acta* **2004**, *1702*, 181–189.

(21) Martinelle, M.; Holmquist, M.; Clausen, I. G.; Patkar, S.; Svendsen, A.; Hult, K. The role of Glu87 and Trp89 in the lid of Humicola lanuginosa lipase. *Protein Eng.* **1996**, *9*, 519–524.

(22) Derewenda, U.; Swenson, L.; Wei, Y.; Green, R.; Kobos, P.; Joerger, R.; Haas, M.; Derewenda, Z. Conformational lability of lipases observed in the absence of an oil-water interface: crystallographic studies of enzymes from the fungi Humicola lanuginosa and Rhizopus delemar. *J. Lipid Res.* **1994**, *35*, 524–534.

(23) Brzozowski, A. M.; Savage, H.; Verma, C. S.; Turkenburg, J. P.; Lawson, D. M.; Svendsen, A.; Patkar, S. Structural origins of the interfacial activation in Thermomyces (Humicola) lanuginosa lipase. *Biochemistry* **2000**, *39*, 15071–15082.

(24) Hedin, E. M.; Høyrup, P.; Patkar, S. A.; Vind, J.; Svendsen, A.; Hult, K. Implications of surface charge and curvature for the binding orientation of Thermomyces lanuginosus lipase on negatively charged or zwitterionic phospholipid vesicles as studied by ESR spectroscopy. *Biochemistry* **2005**, *44*, 16658–16671.

(25) Skjold-Jørgensen, J.; Bhatia, V. K.; Vind, J.; Svendsen, A.; Bjerrum, M. J.; Farrens, D. The Enzymatic Activity of Lipases Correlates with Polarity-Induced Conformational Changes: A Trp-Induced Quenching Fluorescence Study. *Biochemistry* **2015**, *54*, 4186–4196.

(26) Stobiecka, A.; Wysocki, S.; Brzozowski, A. Fluorescence study of fungal lipase from Humicola lanuginosa. *Journal of Photochemistry and Photobiology B: Biology* **1998**, *45*, 95–102.

(27) Yapoudjian, S.; Ivanova, M. G.; Brzozowski, A. M.; Patkar, S. A.; Vind, J.; Svendsen, A.; Verger, R. Binding of Thermomyces (Humicola) lanuginosa lipase to the mixed micelles of cis-parinaric acid/NaTDC. *Eur. J. Biochem.* **2002**, *269*, 1613–1621.

(28) Peters, G. H.; Toxvaerd, S.; Olsen, O.; Svendsen, A. Computational studies of the activation of lipases and the effect of a hydrophobic environment. *Protein Eng.* **1997**, *10*, 137–147.

(29) Gunasekaran, K.; Ma, B.; Nussinov, R. Triggering loops and enzyme function: identification of loops that trigger and modulate movements. *J. Mol. Biol.* **2003**, *332*, 143–159.

(30) Brady, L.; Brzozowski, A. M.; Derewenda, Z. S.; Dodson, E.; Dodson, G.; Tolley, S.; Turkenburg, J. P.; Christiansen, L.; Huge-Jensen, B.; Norskov, L. A serine protease triad forms the catalytic centre of a triacylglycerol lipase. *Nature* **1990**, *343*, 767–770.

(31) Johnson, Q. R.; Nellas, R. B.; Shen, T. Solvent-dependent gating motions of an extremophilic lipase from Pseudomonas aeruginosa. *Biochemistry* **2012**, *51*, 6238–6245.

(32) Kamal, M.; Yedavalli, P.; Deshmukh, M. V.; Rao, N. M. Lipase in aqueous-polar organic solvents: Activity, structure, and stability. *Protein Sci.* **2013**, *22*, 904–915.

(33) Mattos, C.; Bellamacina, C. R.; Peisach, E.; Pereira, A.; Vitkup, D.; Petsko, G. A.; Ringe, D. Multiple solvent crystal structures: probing binding sites, plasticity and hydration. *J. Mol. Biol.* **2006**, *357*, 1471–1482.

(34) Tanaka, A. Differential scanning calorimetric studies on the thermal unfolding of pseudomonas cepacia lipase in the absence and presence of alcohols. *J. Biochem. (Tokyo)* **1998**, *123*, 289–293.

(35) Li, C.; Tan, T.; Zhang, H.; Feng, W. Analysis of the conformational stability and activity of candida antarctica lipase B in organic solvents insight from molecular dynamics and quantum mechanics/simulations. *J. Biol. Chem.* **2010**, *285*, 28434–28441.

(36) Park, H. J.; Joo, J. C.; Park, K.; Kim, Y. H.; Yoo, Y. J. Prediction of the solvent affecting site and the computational design of stable Candida antarctica lipase B in a hydrophilic organic solvent. *J. Biotechnol.* **2013**, *163*, 346–352.

(37) Li, L.; Jiang, Y.; Zhang, H.; Feng, W.; Chen, B.; Tan, T. Theoretical and experimental studies on activity of Yarrowia lipolytica lipase in methanol/water mixtures. *J. Phys. Chem. B* **2014**, *118*, 1976–1983.

(38) Plechkova, N. V.; Seddon, K. R. Applications of ionic liquids in the chemical industry. *Chem. Soc. Rev.* **2008**, *37*, 123–150.

(39) Kirchner, B.; Hollóczki, O.; Canongia Lopes, J. N.; Pádua, A. A. Multiresolution calculation of ionic liquids. *WIREs Comput. Mol. Sci.* **2015**, *5*, 202–214.

(40) Lozano, P. Enzymes in neoteric solvents: From one-phase to multiphase systems. *Green Chem.* **2010**, *12*, 555–569.

(41) Klibanov, A. M. Improving enzymes by using them in organic solvents. *Nature* **2001**, *409*, 241–246.

(42) Weingärtner, H.; Cabrele, C.; Herrmann, C. How ionic liquids can help to stabilize native proteins. *Phys. Chem. Chem. Phys.* **2012**, *14*, 415–426.

(43) Palomo, J. M.; Fuentes, M.; Fernández-Lorente, G.; Mateo, C.; Guisan, J. M.; Fernández-Lafuente, R. General trend of lipase to self-assemble giving bimolecular aggregates greatly modifies the enzyme functionality. *Biomacromolecules* **2003**, *4*, 1–6.

(44) Kaar, J. L.; Jesionowski, A. M.; Berberich, J. A.; Moulton, R.; Russell, A. J. Impact of ionic liquid physical properties on lipase activity and stability. *J. Am. Chem. Soc.* **2003**, *125*, 4125–4131.

(45) Burney, P. R.; Nordwald, E. M.; Hickman, K.; Kaar, J. L.; Pfaendtner, J. Molecular dynamics investigation of the ionic liquid/enzyme interface: Application to engineering enzyme surface charge. *Proteins: Structure, Function, and Bioinformatics* **2015**, *83*, 670–680.

(46) Nordwald, E. M.; Armstrong, G. S.; Kaar, J. L. NMR-guided rational engineering of an ionic-liquid-tolerant lipase. *ACS Catal.* **2014**, *4*, 4057–4064.

(47) Nordwald, E. M.; Kaar, J. L. Stabilization of enzymes in ionic liquids via modification of enzyme charge. *Biotechnol. Bioeng.* **2013**, *110*, 2352–2360.

(48) Jia, R.; Hu, Y.; Liu, L.; Jiang, L.; Zou, B.; Huang, H. Enhancing catalytic performance of porcine pancreatic lipase by covalent modification using functional ionic liquids. *ACS Catal.* **2013**, *3*, 1976–1983.

(49) De Diego, T.; Lozano, P.; Gmouh, S.; Vaultier, M.; Iborra, J. L. Understanding structure-stability relationships of candida antartica lipase B in ionic liquids. *Biomacromolecules* **2005**, *6*, 1457–1464.

(50) Soares, C. M.; De Castro, H. F.; De Moraes, F. F.; Zanin, G. M. Characterization and utilization of Candida rugosa lipase immobilized on controlled pore silica. *Appl. Biochem. Biotechnol.* **1999**, *79*, 745–757.

(51) Dhake, K. P.; Qureshi, Z. S.; Singhal, R. S.; Bhanage, B. M. Candida antarctica lipase B-catalyzed synthesis of acetamides using [BMIM(PF_6)] as a reaction medium. *Tetrahedron Lett.* **2009**, *50*, 2811–2814.

(52) Nandini, K.; Rastogi, N. Liquid–liquid extraction of lipase using aqueous two-phase system. *Food and Bioprocess Technology* **2011**, *4*, 295–303.

(53) Kaar, J. L. Lipase activation and stabilization in room-temperature ionic liquids. *Enzyme Stabilization and Immobilization: Methods and Protocols* **2011**, 25–35.

(54) van Rantwijk, F.; Sheldon, R. A. Biocatalysis in ionic liquids. *Chem. Rev.* **2007**, *107*, 2757–2785.

(55) Hernández-Fernández, F. J.; de los Ríos, A. P.; Lozano-Blanco, L. J.; Godínez, C. Biocatalytic ester synthesis in ionic liquid media. *J. Chem. Technol. Biotechnol.* **2010**, *85*, 1423–1435.

(56) Gamba, M.; Lapis, A. A.; Dupont, J. Supported ionic liquid enzymatic catalysis for the production of biodiesel. *Adv. Synth. Catal.* **2008**, *350*, 160–164.

(57) Sunitha, S.; Kanjilal, S.; Reddy, P.; Prasad, R. Ionic liquids as a reaction medium for lipase-catalyzed methanolysis of sunflower oil. *Biotechnol. Lett.* **2007**, *29*, 1881–1885.

(58) Kamiya, N.; Matsushita, Y.; Hanaki, M.; Nakashima, K.; Narita, M.; Goto, M.; Takahashi, H. Enzymatic in situ saccharification of cellulose in aqueous-ionic liquid media. *Biotechnol. Lett.* **2008**, *30*, 1037–1040.

(59) Zhao, H.; Jones, C. L.; Baker, G. A.; Xia, S.; Olubajo, O.; Person, V. N. Regenerating cellulose from ionic liquids for an accelerated enzymatic hydrolysis. *J. Biotechnol.* **2009**, *139*, 47–54.

(60) Dadi, A. P.; Schall, C. A.; Varanasi, S. *Applied Biochemistry and Biotecnology*; Springer, 2007; pp 407–421.

(61) Dadi, A. P.; Varanasi, S.; Schall, C. A. Enhancement of cellulose saccharification kinetics using an ionic liquid pretreatment step. *Biotechnol. Bioeng.* **2006**, *95*, 904–910.

(62) Deive, F. J.; Ruivo, D.; Rodrigues, J. V.; Gomes, C. M.; Sanromán, M. Á.; Rebelo, L. P. N.; Esperança, J. M.; Rodríguez, A. On the hunt for truly biocompatible ionic liquids for lipase-catalyzed reactions. *RSC Adv.* **2015**, *5*, 3386–3389.

(63) Vrikkis, R. M.; Fraser, K. J.; Fujita, K.; MacFarlane, D. R.; Elliott, G. D. Biocompatible ionic liquids: a new approach for stabilizing proteins in liquid formulation. *J. Biomech. Eng.* **2009**, *131*, 074514.

(64) Chaban, V. V.; Fileti, E. E. Ionic Clusters vs Shear Viscosity in Aqueous Amino Acid Ionic Liquids. *J. Phys. Chem. B* **2015**, *119*, 3824–3828.

(65) Rodrigues, J. V.; Ruivo, D.; Rodríguez, A.; Deive, F. J.; Esperança, J. M.; Marrucho, I. M.; Gomes, C. M.; Rebelo, L. P. N. Structural–functional evaluation of ionic liquid libraries for the design of co-solvents in lipase-catalysed reactions. *Green Chem.* **2014**, *16*, 4520–4523.

(66) Bekker, H.; Berendsen, H.; Dijkstra, E.; Achterop, S.; Van Drunen, R.; Van der Spoel, D.; Sijbers, A.; Keegstra, H.; Reitsma, B.; Renardus, M. Gromacs: A parallel computer for molecular dynamics simulations. Physics computing. 1993; pp 252–256.

(67) Berendsen, H. J.; van der Spoel, D.; van Drunen, R. GROMACS: a message-passing parallel molecular dynamics implementation. *Comput. Phys. Commun.* **1995**, *91*, 43–56.

(68) Lindahl, E.; Hess, B.; Van Der Spoel, D. GROMACS 3.0: a package for molecular simulation and trajectory analysis. *J Mol. Model.* **2001**, *7*, 306–317.

(69) Van Der Spoel, D.; Lindahl, E.; Hess, B.; Groenhof, G.; Mark, A. E.; Berendsen, H. J. GROMACS: fast, flexible, and free. *J. Comput. Chem.* **2005**, *26*, 1701–1718.

(70) Hess, B.; Kutzner, C.; Van Der Spoel, D.; Lindahl, E. GROMACS 4: algorithms for highly efficient, load-balanced, and scalable molecular simulation. *J. Chem. Theory Comput.* **2008**, *4*, 435–447.

(71) Pronk, S.; Páll, S.; Schulz, R.; Larsson, P.; Bjelkmar, P.; Apostolov, R.; Shirts, M. R.; Smith, J. C.; Kasson, P. M.; van der Spoel, D. GROMACS 4.5: a high-throughput

and highly parallel open source molecular simulation toolkit. *Bioinformatics* **2013**, *29*, 845–854.

(72) Martínez, L.; Andrade, R.; Birgin, E. G.; Martínez, J. M. Packmol: A package for building initial configurations for molecular dynamics simulations. *J. Comput. Chem.* **2009**, *30*, 2157–2164.

(73) Vanommeslaeghe, K.; Hatcher, E.; Acharya, C.; Kundu, S.; Zhong, S.; Shim, J.; Darian, E.; Guvench, O.; Lopes, P.; Vorobyov, I. CHARMM general force field: A force field for drug-like molecules compatible with the CHARMM all-atom additive biological force fields. *J. Comput. Chem.* **2010**, *31*, 671–690.

(74) Bjelkmar, P.; Larsson, P.; Cuendet, M. A.; Hess, B.; Lindahl, E. Implementation of the CHARMM force field in GROMACS: Analysis of protein stability effects from correction maps, virtual interaction sites, and water models. *J. Chem. Theory Comput.* **2010**, *6*, 459–466.

(75) Jorgensen, W. L.; Chandrasekhar, J.; Madura, J. D.; Impey, R. W.; Klein, M. L. Comparison of simple potential functions for simulating liquid water. *J. Chem. Phys.* **1983**, *79*, 926–935.

(76) Zhang, Y.; Maginn, E. J. A simple AIMD approach to derive atomic charges for condensed phase simulation of ionic liquids. *J. Phys. Chem. B* **2012**, *116*, 10036–10048.

(77) Mondal, A.; Balasubramanian, S. Quantitative prediction of physical properties of imidazolium based room temperature ionic liquids through determination of condensed phase site charges: a refined force field. *J. Phys. Chem. B* **2014**, *118*, 3409–3422.

(78) Mondal, A.; Balasubramanian, S. A refined all-atom potential for imidazolium-based room temperature ionic liquids: acetate, dicyanamide, and thiocyanate anions. *J. Phys. Chem. B* **2015**, *119*, 11041–11051.

(79) Fileti, E. E.; Chaban, V. V. The scaled-charge additive force field for amino acid based ionic liquids. *Chem. Phys. Lett.* **2014**, *616*, 205–211.

(80) Bussi, G.; Donadio, D.; Parrinello, M. Canonical sampling through velocity rescaling. *J. Chem. Phys.* **2007**, *126*, 014101.

(81) Nosé, S. A molecular dynamics method for simulations in the canonical ensemble. *Mol. Phys.* **1984**, *52*, 255–268.

(82) Hoover, W. G. Canonical dynamics: equilibrium phase-space distributions. *Phys. Rev. A* **1985**, *31*, 1695.

(83) Parrinello, M.; Rahman, A. Polymorphic transitions in single crystals: A new molecular dynamics method. *J. Appl. Phys.* **1981**, *52*, 7182–7190.

(84) Nosé, S.; Klein, M. L. Constant pressure molecular dynamics for molecular systems. *Mol. Phys.* **1983**, *50*, 1055–1076.

(85) Darden, T.; York, D.; Pedersen, L. Particle mesh Ewald: An Nlog(N) method for Ewald sums in large systems. *J. Chem. Phys.* **1993**, *98*, 10089–10092.

(86) Humphrey, W.; Dalke, A.; Schulten, K. VMD: visual molecular dynamics. *J. Mol. Graph.* **1996**, *14*, 33–38.

(87) DeLano, W. L. The PyMOL molecular graphics system. **2002**,

(88) Peters, G. H.; Svendsen, A.; Langberg, H.; Vind, J.; Patkar, S.; Toxvaerd, S.; Kinnunen, P. Active serine involved in the stabilization of the active site loop in the Humicola lanuginosa lipase. *Biochemistry* **1998**, *37*, 12375–12383.

(89) Buxbaum, E. *Fundamentals of protein structure and function*; Springer, 2007; Vol. 31.

(90) Zhu, K.; Jutila, A.; Tuominen, E. K.; Patkar, S. A.; Svendsen, A.; Kinnunen, P. K. Impact of the tryptophan residues of Humicola lanuginosa lipase on its thermal stability. *Biochimica et Biophysica Acta* **2001**, *1547*, 329–338.

(91) Zhu, K.; Jutila, A.; Kinnunen, P. K. Steady state and time resolved effects of guanidine hydrochloride on the structure of Humicola lanuginosa lipase revealed by fluorescence spectroscopy. *Protein Sci.* **2000**, *9*, 598–609.

(92) Ventura, S. P.; Santos, L. D.; Saraiva, J. A.; Coutinho, J. A. Concentration effect of hydrophilic ionic liquids on the enzymatic activity of Candida antarctica lipase B. *World J. Microbiol. Biotechnol.* **2012**, *28*, 2303–2310.

(93) Klähn, M.; Lim, G. S.; Wu, P. How ion properties determine the stability of a lipase enzyme in ionic liquids: A molecular dynamics study. *Phys. Chem. Chem. Phys.* **2011**, *13*, 18647–18660.

(94) Wen, Q.; Chen, J.-X.; Tang, Y.-L.; Wang, J.; Yang, Z. Assessing the toxicity and biodegradability of deep eutectic solvents. *Chemosphere* **2015**, *132*, 63–69.

(95) de María, P. D.; Maugeri, Z. Ionic liquids in biotransformations: from proof-of-concept to emerging deep-eutectic-solvents. *Curr. Opin. Chem. Biol.* **2011**, *15*, 220–225.

(96) Zisis, T.; Freddolino, P. L.; Turunen, P.; van Teeseling, M. C.; Rowan, A. E.; Blank, K. G. Interfacial activation of Candida antarctica lipase B: combined evidence from experiment and simulation. *Biochemistry* **2015**, *54*, 5969–5979.

(97) Verger, R. Interfacial activationof lipases: facts and artifacts. *Trends Biotechnol.* **1997**, *15*, 32–38.

(98) Ha, S. H.; Lan, M. N.; Lee, S. H.; Hwang, S. M.; Koo, Y.-M. Lipase-catalyzed biodiesel production from soybean oil in ionic liquids. *Enzyme Microb. Technol.* **2007**, *41*, 480–483.

(99) Belafi-Bako, K.; Kovacs, F.; Gubicza, L.; Hancsok, J. Enzymatic biodiesel production from sunflower oil by Candida antarctica lipase in a solvent-free system. *Biocatal. Biotransform.* **2002**, *20*, 437–439.

(100) Xu, Y.; Du, W.; Liu, D.; Zeng, J. A novel enzymatic route for biodiesel production from renewable oils in a solvent-free medium. *Biotechnol. Lett.* **2003**, *25*, 1239–1241.

(101) Cajal, Y.; Svendsen, A.; Girona, V.; Patkar, S. A.; Alsina, M. A. Interfacial control of lid opening in Thermomyces lanuginosa lipase. *Biochemistry* **2000**, *39*, 413–423.

Table of Content